Differences in Spiking Patterns Among Cortical Neurons

Shigeru Shinomoto
shinomoto@scphys.kyoto-u.ac.jp
Department of Physics, Graduate School of Science, Kyoto University,
Kyoto 606-8502, Japan

Keisetsu Shima
shimak@mail.cc.tohoku.ac.jp
Jun Tanji
tanjij@mail.cc.tohoku.ac.jp
Department of Physiology, Tohoku University School of Medicine,
Sendai 980-8575, Japan

Spike sequences recorded from four cortical areas of an awake behaving monkey were examined to explore characteristics that vary among neurons. We found that a measure of the local variation of interspike intervals, L_V, is nearly the same for every spike sequence for any given neuron, while it varies significantly among neurons. The distributions of L_V values for neuron ensembles in three of the four areas were found to be distinctly bimodal. Two groups of neurons classified according to the spiking irregularity exhibit different responses to the same stimulus. This suggests that neurons in each area can be classified into different groups possessing unique spiking statistics and corresponding functional properties.

1 Introduction

The basic problem of understanding the mechanisms that govern the working of the brain will ultimately be solved by elucidating the causal relation between anatomical circuitry and physiological function. In addition to general information regarding the nature of a neuron's temporal activity, more specific information that identifies the type and location of the neuron would be useful in elucidating this relation.

With the idea of obtaining such specific information, we can consider the information provided by a recorded spike sequence to be of three types. The first type of information is represented by the gross spike rate. It is known that the firing rate of an interneuron is significantly higher than that of a pyramidal neuron (Ranck, 1973; Buzsaki, Leung, & Vanderwolf, 1983). The second type is constituted by the fine waveform of the action potential. It has been found that there is a significant difference between the action

potential waveforms of interneurons and pyramidal neurons (Csicsvari, Hirase, Czurko, & Buzsaki, 1998; Constantinidis, Williams, & Goldman-Rakic, 2002). The third type consists of the spiking patterns contained in the set of consecutive interspike intervals (ISIs). We suggest in this letter that a more detailed classification of neurons can be realized through a statistical analysis of neuronal spiking characteristics.

In a previous study, we computed the coefficient of variation, C_V, the skewness coefficient, and the correlation coefficient of consecutive intervals of spike sequences and found that their distributions depend strongly on the recording site (Shinomoto, Sakai, & Funahashi, 1999; Sakai, Funahashi, & Shinomoto, 1999; Shinomoto, Shima, & Tanji, 2002). Even for spike rates differing by as much as a factor of three, the distributions of these dimensionless coefficients derived from data recorded from the same area (of different monkeys in different laboratories) exhibit strong similarities. It is thus seen that the distribution of these statistical coefficients is determined by the recording site. But the values of these coefficients observed for a single neuron were found to vary significantly in time. For this reason, these coefficients are not useful for the classification of individual neurons.

Here, we introduce another measure, the local variation of interspike intervals, L_V, which reflects the spiking characteristics intrinsic to individual neurons. It is found that different groups of neurons classified according to L_V values exhibit different characteristic responses, which we term tonic and phasic, to the same stimulus, with a distinct time difference between their response latencies. This kind of classification scheme should provide useful information concerning the type and the intra-areal location of neurons.

2 Statistical Measures C_V and L_V

Neuronal spike sequences recorded from the presupplementary motor area (pre-SMA: area 6), the supplementary motor area (SMA: area 6), the rostral cingulate motor area (CMAr: area 24), and the prefrontal cortical area (PF: area 46) of a monkey performing a waiting period task designed by Shima, Sawamura and Tanji (2001) were examined to determine if we can identify statistical characteristics useful in the classification of neurons. The details of the waiting period task are summarized in appendix A.

From each spike sequence recorded from a neuron, 100 consecutive ISIs were selected, and from these, values of the C_V and the measure of local variation of the interspike intervals, L_V, were computed. The conventional C_V is defined as

$$C_V = \sqrt{\frac{1}{n-1} \sum_{i=1}^{n} (T_i - \overline{T})^2} \Big/ \overline{T}, \tag{2.1}$$

where T_i is the duration of the ith ISI, n is the number of ISIs (in this study $n = 100$), and $\overline{T} = \frac{1}{n} \sum_{i=1}^{n} T_i$ is the mean ISI.

The measure of local variation we introduce here is defined as

$$L_V = \frac{1}{n-1} \sum_{i=1}^{n-1} \frac{3(T_i - T_{i+1})^2}{(T_i + T_{i+1})^2} , \qquad (2.2)$$

in which the summand is proportional to the square of the individual terms of C_{V2}, which was introduced by Holt, Softky, Koch, and Douglas (1996) for the purpose of comparing the temporal ISI randomness of neurons in vitro and in vivo. The factor 3 is taken so that for the Poisson (random) ISI sequence, the expectation value of L_V becomes 1. The expectation values of L_V and C_V for the more general gamma processes are summarized in appendix B.

Both C_V and L_V vanish for a regular ISI sequence in which T_i is constant, and both are expected to be near 1 for a sufficiently long Poisson ISI sequence. The L_V measure reflects the stepwise variability of a spike sequence and is expected to effectively extract the spiking characteristics intrinsic to individual neurons, even for cases in which the spike rate is externally modulated. For a spike sequence that is locally quasi-regular but globally modulated, L_V assumes a small value, while C_V assumes a large value. The simple correlation between consecutive ISIs is not as efficient as L_V for the purpose of extracting intrinsic characteristics. The mean value of C_{V2} has properties similar to those of L_V. However, here we employ L_V because we found that it elucidates differences among the degrees of intrinsic spiking randomness of neurons more effectively than the other measures.

We also applied those statistical measures to the doubly stochastic processes in which the spike rate of the Poisson process is temporally modulated according to the Ornstein-Uhlenbeck process (see, e.g., Shinomoto & Tsubo, 2001) and confirmed that L_V does not undergo a large change, while C_V undergoes a significant change according to the spike rate modulation. Tiesinga, Fellous, & Sejnowski (2002) showed that in vitro neurons and leaky integrate-and-fire model neurons driven by fluctuating stimuli do not produce Poisson spike trains; rather, the ISIs are correlated. The exhaustive examination of how such structures reflect to the L_V values would constitute another theoretical study. We would like to confine ourselves in this study to the demonstration of the effectiveness of L_V in classifying in vivo neurons.

3 Classification of Neurons According to L_V Values

The histograms of the C_V and L_V values obtained for the spike sequences recorded from the four areas under consideration are plotted in Figure 1. It is seen that each C_V distribution has a long tail extending to the right and possesses only a single peak. By contrast, the L_V distributions are compact,
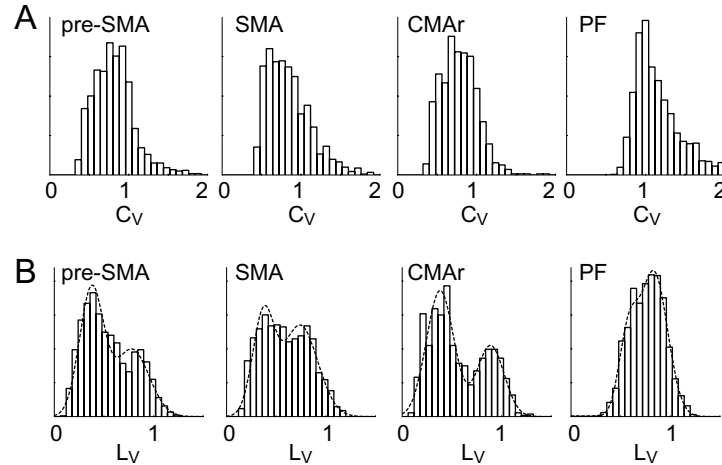
Figure 1: Normalized histograms of the values of C_V and L_V for the four corti-
cal areas considered. While the C_V distributions each exhibit only single peaks,
the L_V histograms for the pre-SMA, SMA, and CMAr areas exhibit two dis-
tinct peaks. The dashed curves that overlay the L_V histograms represent the
two-component gaussian mixture distributions fitted to the data. The centers
of the two components of the distribution determined by using the maximum
likelihood method in the pre-SMA, SMA, CMAr, and PF areas are, respectively,
{0.38, 0.78}, {0.37, 0.74}, {0.38, 0.89}, and {0.58, 0.83}.

and those for three of the four areas possess two distinct peaks. We fit
two-component gaussian mixture distributions to these L_V data sets (see
appendix C). For the resulting fitted distributions, the peaks centered at
the larger value of L_V for all four are positioned closely, while the peaks
centered at the smaller value of L_V for three (those for the pre-SMA, SMA,
and CMAr) are positioned closely. In the pre-SMA, SMA, and CMAr of the
medial frontal cortex, the two peaks obtained in this fit are distinct and well
separated. This result suggests that the neurons in these areas can largely
be classified into two types: type A neurons, which generate irregular spike
sequences (with large values of L_V), and type B neurons, which generate
quasi-regular spike sequences (with small values of L_V).

In the classification scheme we employ, we use this two-component gaus-
sian fit, and with it we determine a cutoff value of L_V that defines the clas-
sification boundary: all neurons for which the measured value is above and
below this boundary are classified, respectively, as type A and type B. Be-
cause of the qualitative difference in the data for the PF in comparison with
the other three areas, we consider these two cases separately. First, we con-
sider the pre-SMA, SMA, and CMAr in the medial frontal cortex (indicated
by MF in the figures). For simplicity, we use the same classification cutoff

value of L_V for each of these three areas, and for this reason, we combined the data for all three and carried out the two-component gaussian fit (see Figure 2A). The two components of the distribution obtained in this fit are centered at 0.81 and 0.38, with weights 0.43 and 0.57, and have standard deviations 0.16 and 0.13. We assume that classification cutoff value θ is given so as to minimize the total areas of the two gaussian tails that are on the "wrong" sides, referenced to the cutoff θ. This is mathematically identical to seeking the value of L_V at which the two component distributions balance. In our case, $\theta = 0.59$, and with this value, the misclassification percentage is 6.9% (see Figure 2B). This optimal cutoff determined through a complicated procedure is very close to the simple midpoint of the centers of the two components, $(0.81 + 0.38)/2 = 0.60$. It should be noted that the cutoff value does not change greatly even if we determine it independently for each of the three areas in the MF (in which case, $\theta = 0.58$ for the pre-SMA, 0.52 for the SMA, and 0.66 for the CMAr), and all the results given below are altered very little in response to small changes of the cutoff value. We evaluated the values of L_V of 3506 sequences of 100 ISIs recorded from 83 neurons in these three areas of the medial frontal cortex. We define the "true" value of L_V for a given neuron by the average of L_V obtained from sequences recorded from the neuron. If the L_V of an individual sequence lies on the same side of the neuron's mean L_V as the "true" value, referenced to the cutoff θ, this sequence is regarded as having yielded a correct classification; if it lies on the opposite side, it is regarded as having yielded an incorrect classification (see Figure 2C). The empirical misclassification percentage evaluated in this manner was 9.7%. This means that the neurons in these medial frontal cortical areas could be correctly classified into the two types from spike sequences containing only 100 ISIs with a reliability of greater than 90%.

Although the distribution of L_V values for the PF area is not distinctly bimodal, for the sake of comparison, we carried out the same procedure to determine the classification boundary θ' for the PF data (see Figure 2D). In this case, two components of the gaussian mixture distributions are centered at 0.83 and 0.58, with weights 0.73 and 0.27 and standard deviations 0.14 and 0.09. The optimal cutoff value was found to be $\theta' = 0.66$, and with this, the misclassification percentage was 12.3% (see Figure 2E). For the PF data, the optimal cutoff was slightly smaller than the simple midpoint of the centers of the two components, $(0.83 + 0.58)/2 = 0.71$. However, the results obtained from the cutoff classification were found to be insensitive to this amount of change of the cutoff. With the cutoff value $\theta' = 0.66$, we counted the number of empirically defined misclassified sequences among 1672 sequences of 100 ISIs recorded from 28 neurons in the PF. The empirical misclassification percentage for the PF data was 16.8%, larger than that for the medial frontal cortex.

Individual components of these data-fitted mixture distributions have standard deviations ranging from 0.09 to 0.16 (see Figure 2). In order to
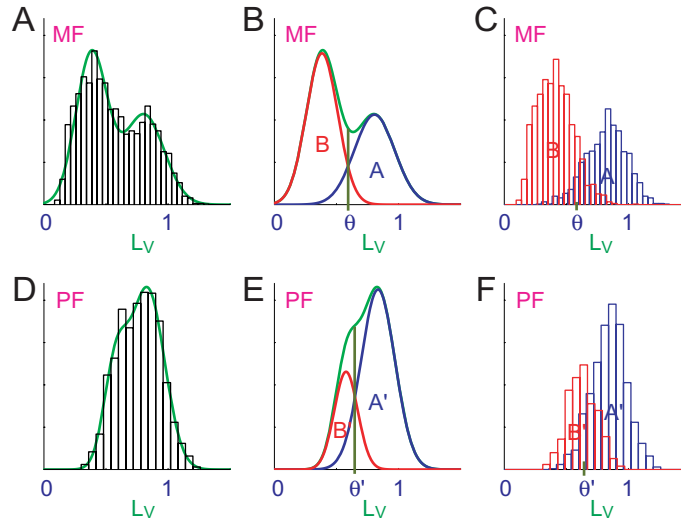
examine whether this amount of standard deviation could arise naturally across different realizations of 100 ISIs, we performed a numerical simulation to estimate the standard deviations of the L_V values for the Poisson process in which n event intervals are independently drawn from exponential distribution. The standard deviation of the L_V values is found to scale as $1/\sqrt{n}$. In the case $n = 100$, the standard deviation is about 0.10. There is some room to find the finer categorization scheme from the L_V distribution
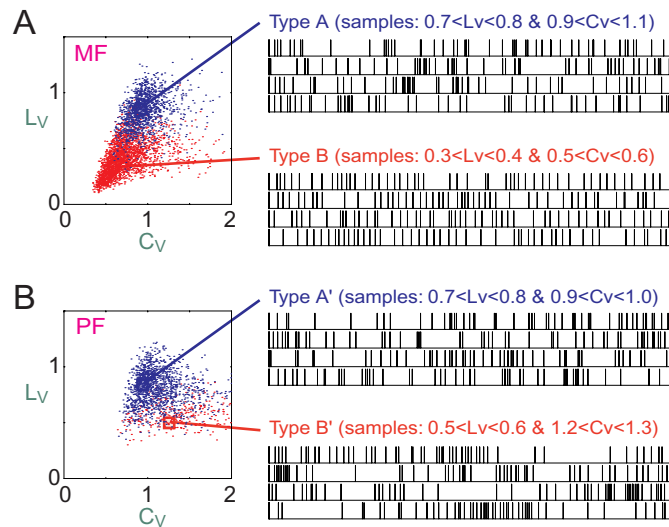
Figure 2: *Facing page*. Categorization of ISI sequences. (A) Normalized histogram of the values of L_V for all 3506 sequences recorded from the pre-SMA, SMA, and CMAr. (B) The two components of the gaussian mixture fit to the data are centered at 0.38 and 0.80. The classification cutoff $\theta = 0.59$ minimizes the total area of gaussian tails that are on the "wrong" side, and with it the misclassification percentage is 6.9%. (C) Histograms of data classified according to neurons' mean values of L_V. The empirical percentage of misclassified sequences (in which case, a neuron's mean value of L_V is greater than θ, while the value of L_V for individual sequence considered is less than θ, or vice versa) is 9.7% for $\theta = 0.59$. (D) Normalized histogram of the values of L_V for 1672 sequences recorded from the PF. (E) The two components of the gaussian mixture fit to the data are centered at 0.58 and 0.83. The classification cutoff $\theta = 0.66$ minimizes the total areas of gaussian tails that are on the "wrong" side, and in this case, the misclassification percentage is 12.3%. (F) Histograms of data classified according to neurons' mean values of L_V. The empirical percentage of misclassification is 16.8% for $\theta = 0.66$.

if much longer spike sequences are used, but for the 100 ISIs, the component resolution level (0.09–0.16) we obtained is evaluated to be nearly optimal.

4 Correlation Between C_V and L_V

Here we wish to elucidate the relation between the C_V and L_V values computed for a single sequence of 100 ISIs. The scattergrams of (C_V, L_V) values computed for the three areas in the medial frontal cortex (MF) and for the prefrontal cortex (PF) are depicted in Figures 3A and 3B. The correlation coefficients for the MF and PF data are, respectively, $r = 0.53$ and $r = -0.22$, both of which are statistically insignificant: knowledge of the C_V value of a sequence does not provide significant information concerning the L_V value of the same sequence. In Figures 3A and 3B, (C_V, L_V) points obtained from sequences generated by the two types of neurons have different colors. It is seen from these figures that the classical C_V measure is ineffective for the present cell-type classification. Typical spike sequences sampled from type A and type B neurons in the MF and type A' and type B' neurons in the

Figure 3: *Facing page*. Scattergrams of (C_V, L_V) values each computed for single sequences recorded from (A) the three areas in the medial frontal cortex, MF, and (B) the prefrontal cortex, PF. The correlation coefficients of the distributions are, respectively, $r = 0.53$ and $r = -0.22$, both statistically insignificant. The (C_V, L_V) points for the sequences generated from type A (A') and type B (B') neurons are, respectively, colored blue and red. Raster diagrams of 50 ISIs sampled from type A (A') and B (B') neurons are also shown.

PF are also depicted as raster diagrams for 50 ISIs in Figure 3. Note that 50 ISIs were used for the purpose of demonstration only, while all the analyses were carried using 100 consecutive ISIs.

Any measure that does not vary significantly over the different spike sequence taken from any given neuron in comparison with the variations among the sequences taken from different neurons could be regarded as representing a certain intrinsic property of the individual neurons. The standard deviations of the C_V and L_V values computed for all ISI sequences recorded from all neurons are, respectively, 0.34 and 0.26, and the mean standard deviations measured for individual neurons are, respectively, 0.20 and 0.10. The small deviations of L_V values for individual neurons imply that this measure is intrinsic to individual neurons.

To see the amount by which the measures C_V and L_V vary over time, we plotted the scattergrams for a pair of C_V values and a pair of L_V values evaluated for two spike sequences selected randomly from a single neuron (see Figure 4). We find that the corresponding correlation coefficients r computed for the four areas are also displayed in those figures. The values of C_V exhibit weak correlation ($r = 0.49 - 0.59$) for the pre-SMA, SMA, and CMAr and very weak correlation ($r = 0.27$) for the PF. In contrasting, the values of L_V exhibit strong correlation ($r = 0.78 - 0.85$) for the pre-SMA, SMA, and CMAr and moderate correlation for the PF ($r = 0.59$). Those strong correlations of the L_V values also indicate that the characteristic represented by the value of L_V is intrinsic to individual neurons.
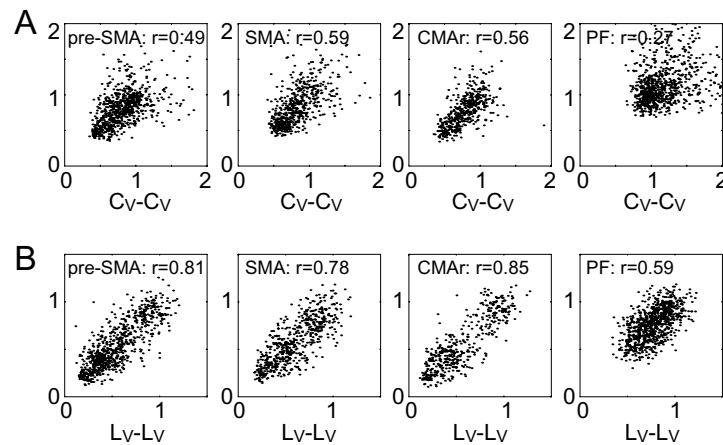

Figure 4: Scattergrams of the values of C_V and the values of L_V for two sequences of 100 ISIs, each generated by the same neuron. The correlation coefficient is denoted by r. Large r values of the L_V scattergrams imply that the neuron always exhibits similar values of L_V.

5 Event-Related Activity of Two Groups of Neurons

In the next step, we considered the possibility that neurons belonging to type A and type B may exhibit different properties of activity in response to external stimuli. For this reason, we examined neuronal responses to a visual signal (a light-emitting diode, LED) used as an instruction signal in the waiting period task considered here. As confirmed above, we were able to carry out the classification with high reliability using only 100 ISIs, and in this way, individual spike sequences were categorized as type A and type B. In order to increase the reliability further, we also classified each neuron according to the mean value of L_V. Figure 5 represents the peri-event population histograms aligned at the onset of the LED signal for the classified groups of neurons in the four areas (see appendix D).

We first consider the pre-SMA (see Figure 5A). Among the four areas studied, the pre-SMA is known to contain the largest concentration of neurons that exhibit different levels of cue period activity strongly correlated to the length of the waiting period (Shima et al., 2001). In the peri-event population histogram of Figure 5A, neurons in the pre-SMA exhibit clear and distinct responses to the cue LED. The group of type A neurons in this area reach the activity level of tonic firing within 200 to 300 msec after the light is turned on and sustain this activity throughout 2000 msec and even after the light is turned off at 2000 msec. By contrast, the mean activity of type B neurons in this area is (relatively) phasic, reaching a maximum within 150 to 200 msec after the light is turned on and then beginning to relax after 500 to 600 msec while the light remains on. It is notable that there is a significant time difference between the latencies of the responses of the two groups. We fitted piecewise linear functions to the type A and type B data by means of the maximum likelihood method to determine the transition times over which the spike rate starts to change (see appendix E). With these, the time difference of the response latencies was determined to be 88 msec (see Figure 6A). It is also seen from Figures 6B through 6E that the response latencies of type A and type B neurons do not change owing to the choice of the waiting period. It may not be possible to account for this large time difference between the latencies in terms of the characteristics of single neurons, and therefore it may be the case that these two groups of neurons are receiving different signals.

We next consider the SMA (see Figure 5B) and CMAr (see Figure 5C). Though the L_V distributions of the SMA and CMAr are in some sense similar to that of the pre-SMA, they are functionally different. For the waiting period task, Shima et al. (2001) observed that few neurons in these areas exhibit statistically significant dependence of cue period activity on the length of the waiting period. As seen in the peri-event population histograms, neither the SMA nor CMAr exhibits prominent responses to the cue LED. It is interesting that in the SMA, type A and type B groups exhibit distinctly different time evolutions. This also suggests that these two groups of neurons
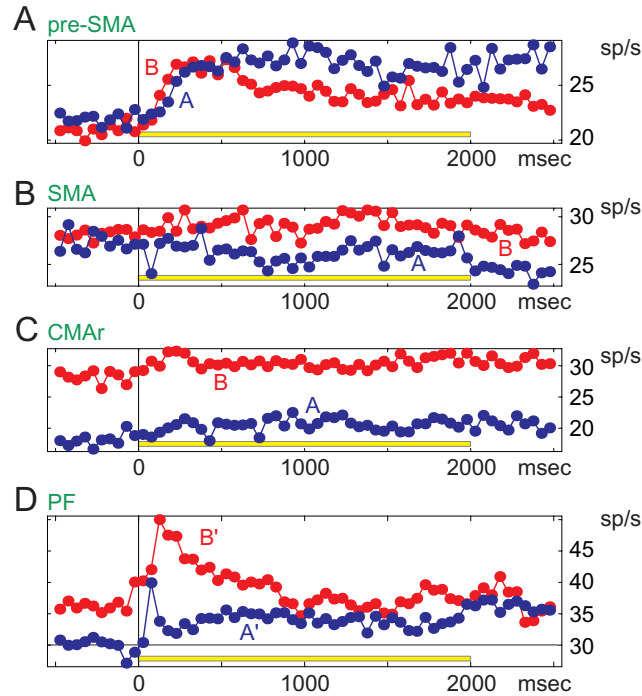
Figure 5: Population histograms aligned at the onset of the visual stimulus (LED). (A) Neurons in the pre-SMA exhibit a prominent response to the cue LED. Type A neurons gradually approach the tonic level and sustain this activity even 2000 msec after the LED is turned off. By contrast, the mean activity of type B neurons is relatively quickly appearing and phasic (gradually decaying). The time difference between the latencies of type B and type A neurons implies that they receive different signals and have different functional roles. (B, C) Neurons in the SMA and CMAr do not exhibit prominent responses to the LED stimulus for the task. (D) In the PF, although the L_V distribution is not distinctly bimodal, type A' and type B' neurons exhibit distinctly different types of time evolution. Some type A' neurons exhibit quickly appearing and quickly decaying responses to the onset of the light signal. After this transient response has ceased, type A' neurons maintain tonic levels of firing even after the LED is turned off. By contrast, the mean activity of type B' neurons is phasic.

act in different ways. However, the role of this area in the waiting period task is unknown. In the CMAr, the two groups exhibit different mean spike rates, but neither exhibits a prominent response in task considered here. The functional difference between type A and type B neurons cannot be investigated in the absence of prominent temporal change. In other words, these areas are irrelevant to the task considered here. It is there-
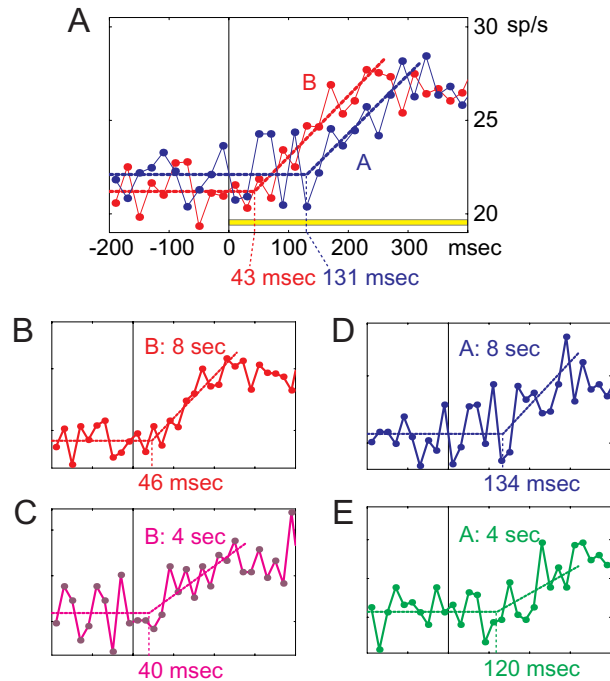
Figure 6: (A) Piecewise linear functions fitted to the time evolutions of the spike rates of type A and type B groups of neurons in the pre-SMA. In this figure, peri-event time histograms are plotted with a bin size of 20 msec. The transition times over which the spike rates start to change are estimated as 131 ± 14 msec and 43 ± 14 msec at a significance level of 0.05 for type A and type B groups of neurons, respectively. (B–E) Type A and type B data subclassified according to the waiting period 8 and 4 sec. The transition times are estimated as 46 ± 15 msec for the type B sequences with the waiting period of 8 sec, 40 ± 27 msec for type B of 4 sec, 134 ± 22 msec for type A of 8 sec, and 120 ± 31 msec for type A of 4 sec. The latencies do not change according to the choice of the waiting period, while those of type A data and type B data are kept mutually distinguishable.

fore desirable to study other tasks in which the areas exhibit prominent responses.

Finally, we consider the PF (see Figure 5D). Few neurons in this area exhibit statistically significant dependence of cue period mean activity on the length of the waiting period. However, the neurons in the PF are found to exhibit clear and distinct responses to the cue LED. We classified neurons for which the mean value of L_V is greater than $\theta = 0.59$ as type A′ and otherwise as type B′. The qualitative features of the following results obtained using $\theta' = 0.66$ are essentially the same as those obtained using $\theta' = 0.71$, which

is the simple midpoint of the positions of the two subdistributions. We found that some type A′ neurons exhibit a quickly appearing and quickly decaying transient in response to the onset of the light signal, with a latency of about 50 msec. However, other than this transient response of some type A′ neurons , the qualitative features of all type A′ and type B′ neurons in the PF are similar to those of type A and type B neurons, respectively, in the pre-SMA. Type A′ neurons sustain tonic activity throughout 2000 msec and even after the light is turned off, and type B′ neurons exhibit phasic response, and the activity begins to relax (after 200–300 msec in this case) while the LED remains on. The increment of the mean spike rate of the type A′ neurons, which is tonically sustained in the waiting period, is about 4 to 5 spikes per second, which is comparable to that of the type A neurons in the pre-SMA.

Though the L_V distributions in the pre-SMA and PF differ significantly, neurons classified into groups according to whether $L_V > \theta$ (or θ') or $L_V \leq \theta$ (or θ') have common characteristics: type A and type A′ neurons (with large L_V) exhibit tonic activity, while type B and type B′ neurons (with small L_V) exhibit phasic responses. It is worthwhile to examine whether these correspondences are observed in other areas also.

The time difference between the response latencies of the type A and type B neurons in the pre-SMA and the difference between temporal activity changes of type A′ and type B′ neurons in the PF suggest that the classification scheme according to the L_V measure is effective for detecting the intra-areal information flow. It should be noted that the latencies of the two or more groups of neurons could depend on the area, because the response latencies are determined by the signal transmission channels specific to each area. The distributions of L_V values for the SMA and CMAr are distinctly bimodal, but the neurons in those areas exhibit no prominent responses to the waiting period task. They may exhibit prominent responses in the other kind of tasks. Functional differences between groups of neurons could be determined for the cases in which neurons are responsive.

6 Discussion

We have verified that the local variation, L_V, represents a good measure for categorizing neurons. In particular, the classification of neurons according to their values of L_V succeeds in separating them into groups possessing distinct functional natures, as evidenced by our finding that neurons in different groups exhibit different responses to external stimuli. Once the cutoff value of L_V is determined, the classification can be carried out as a simple on-line process, in which the type of a neuron, type A or type B (or type A′ or type B′), is determined from a single sequence of ISIs. We propose that physiologists reexamine their experimental data with the use of statistical quantities characterizing spike sequences, like L_V, to classify neuron types as a step toward opening a new avenue of investigation.

The problem we now face is to determine how the spiking categories correspond to neuroanatomical categories of the neurons. The most fundamental neuroanatomical categories are those of pyramidal neurons and interneurons. One may therefore guess that these correspond to our types A and B (or A′ and B′). However the type A and type B neurons we have identified do not exhibit such large differences in spike rates as would be expected for these neurons (except in the cases of the CMAr, in which there was a certain difference). Presumably, the standard single glass-insulated microelectrode rarely detects the depolarization signals of small interneurons. Our types A and B may represent subclasses of the pyramidal neurons. It is equally likely that the differences in the ISI characteristics are due to the statistical characteristics of the input signals to the neurons.

By fitting two-component gaussian distributions to the L_V data sets, we found that the data obtained from the pre-SMA, SMA, and CMAr in the medial frontal cortex MF are similar, and those obtained from the PF differ significantly. It is interesting that the categorization of these areas according to the shape of the L_V distribution is the same as their cytoarchitectural classification, according to which the PF is called a "granular region," while the pre-SMA, SMA, and CMAr are called the "agranular regions" (Garey, 1999; Parent, 1996). These cytoarchitectural terms are derived from the presence and absence of a thick granular layer IV. It is unlikely, however, that the spiking signals of granule cells play a major role in determining the shape of the L_V distribution, because for the L_V distributions, the three agranular regions that do not contain many granule cells possess distinct peaks centered at small values of $L_V \approx 0.4$, while that for the granular region PF, which contains many granule cells, does not possess a distinct peak near the same position. The neurons studied using the recording method are most likely pyramidal neurons, which are mainly located in layers II, III and V. It may be that the present classification into type A and type B for the MF (the pre-SMA, SMA, and CMAr) and type A′ and type B′ for the PF corresponds to different layer of neurons. It is desirable to examine this conjecture using different kinds of experiments.

Appendix A: Waiting Period Task of Shima et al. (2001)

Here we review the waiting period task designed by Shima et al. (2001), for which our analysis was applied. The task was performed by a monkey (*Macaca fuscata*), which was cared for according to the NIH Guidelines for the Care and Use of Laboratory Animals. This task consists of consecutive blocks of five to seven repeated trials. Each trial starts when the monkey presses a key. After the monkey has pressed the key for 1 to 2 sec, one of three colored LEDs illuminates for 2 sec. In order to complete a trial successfully, the monkey is required to continue pressing the key for an interval longer than some predetermined period of 2, 4, or 8 sec (including the time that

the LED is on). This predetermined period is the same for all trials within a given block and is uniquely determined by the combination of the color of the LED illuminated for 2 sec at the beginning of each trial in question (which is the same for all the trials in the same block) and whether there was simultaneous illumination of three LEDs at the beginning of the block of trials. The monkey is rewarded with a drop of juice after every successfully completed trial. If the monkey fails (it releases the key before the end of the assigned period), it is not rewarded, and the same trial is repeated. The minimum number of trials repeated in each block is five, but in certain cases, the number of trials became six or seven due to the monkey's failure. The entire experiment consists of repeated blocks of five to seven trials, with the waiting time for each block chosen randomly.

Neuronal activity was recorded from the pre-SMA, SMA, CMAr, and PF areas while the animal was performing the trained task (Shima & Tanji, 2000). Extracellular recordings of single-cell discharges were made using a standard technique of transdural recording (Evarts, 1968). Glass-insulated Elgiloy-alloy microelectrodes, with impedances of 1.5 to 3 MΩ (measured at 1 KHz) were used. Single-cell discharges were collected using a window discriminator that produced a pulse for each valid spike that met both amplitude and time constraints (Bak & Scmidt, 1977). Extreme care was taken to sort out spikes belonging to a single cell, avoiding spurious contamination of spikes from other cells. This was confirmed by real-time, high-speed monitoring of neuronal spikes on a computer display, which were triggered by each sorted pulses.

The pre-SMA, SMA, and CMAr are higher-order motor areas in the medial frontal cortex involved in guiding motor behavior (Tanji, 1996), while the PF is believed to play a major role in behavioral supervision, problem solving, and short-term memory (Fuster, 1997). A number of neurons in each of the areas studied were found to continue to display high levels of activity during waiting periods. In computing statistical measures, we set the standard for the number of ISIs as 100; sequences containing fewer than 100 spikes were dismissed. In the analysis, we ignored all data taken from trials with a 2 sec waiting period, in which 100 ISIs were rarely found. For each 4 or 8 sec waiting period considered, if the total number of spikes exceeded 100, we selected the centrally located 100 consecutive ISIs to compute the statistical measures of interest. The numbers of independent neurons recorded in the pre-SMA, SMA, CMAr, and PF are, respectively, 42, 36, 35, and 28, and the numbers of sequences of 100 consecutive ISIs obtained in total for each of these areas are, respectively, 1485, 1132, 889, and 1672.

Appendix B: Expectation Values of L_V and C_V for the Gamma Processes

We first show that the L_V defined in equation 2.2 is expected to be 1 for the Poisson ISI sequence, in which T_i and T_{i+1} are drawn independently from

the exponential distribution function,

$$p(T) = a \exp(-aT). \tag{B.1}$$

The expectation value of

$$3 \frac{(T_i - T_{i+1})^2}{(T_i + T_{i+1})^2} \tag{B.2}$$

for the Poisson process is given as

$$\int_0^\infty dt_1 \int_0^\infty dt_2 \, 3 \frac{(t_1 - t_2)^2}{(t_1 + t_2)^2} \exp(-t_1 - t_2). \tag{B.3}$$

This integration can be carried out with the transformation from $\{t_1, t_2\}$ to $\{x, y\} = \{(t_1 + t_2)/2, (t_1 - t_2)\}$ as

$$\int_0^\infty dx \int_{-2x}^{2x} dy \, 3 \frac{y^2}{(2x)^2} \exp(-2x) = 1. \tag{B.4}$$

Next, we would like to compute the expectation values of L_V and C_V for a more general renewal process such as represented by the gamma distribution of ISIs,

$$p_z(T) = a^z T^{z-1} \exp(-aT)/\Gamma(z), \tag{B.5}$$

where $\Gamma(z)$ is the gamma function,

$$\Gamma(z) = \int_0^\infty dt \, t^{z-1} \exp(-t). \tag{B.6}$$

The gamma distribution for the natural number z corresponds to the accumulated Poisson process, in which the neuron generates spikes when the number of incoming Poisson (random) inputs reaches z. The original Poisson process corresponds to $z = 1$. The expectation value of L_V for the gamma distribution of the general order z can also be obtained analytically by means of the same transformation,

$$\langle L_V \rangle = \frac{3}{2z + 1}, \tag{B.7}$$

where $< \ldots >$ represents the average operation with respect to the given distribution. The expectation value of C_V is easily computed for the gamma distribution,

$$\langle C_V \rangle = \frac{1}{\sqrt{z}}. \tag{B.8}$$

We summarize in Figure 7 how the expectation values of C_V and L_V change according to the order z of the gamma distribution functions.
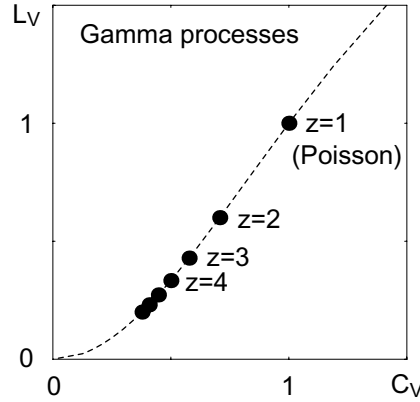
Figure 7: The expectation values of L_V and C_V for the gamma processes represented by the family of distribution functions $p_z(T) = a^z T^{z-1} \exp(-aT)/\Gamma(z)$.

Appendix C: Gaussian Mixture Distribution

We fit two-component gaussian mixture distributions to the L_V values of the data sets for each area to determine the distribution characteristics. The m-component gaussian mixture distribution is defined as

$$p(x) = \sum_{k=1}^{m} w_k N(x|\mu_k, \sigma_k^2), \tag{C.1}$$

where $N(x|\mu, \sigma^2)$ is the gaussian (normal) distribution of mean μ and variance σ^2, and $w_k(> 0)$ is the weight of the kth component distribution, with $\sum_{k=1}^{m} w_k = 1$. This distribution is fitted to a data set $\{x_1, x_2, \cdots, x_P\}$ by locally maximizing the log likelihood,

$$\ell = \sum_{j=1}^{P} \ln p(x_j), \tag{C.2}$$

with respect to all w_k, μ_k, and σ_k^2. The theoretical reason that we used two-component distributions ($m = 2$) is explained in the following.

If we wish to compare distribution functions with different numbers of parameters, the goodness of the fit represented by the log-likelihood ℓ is not sufficient. In the standard model selection criterion, the Akaike Information Criterion, a model distribution is penalized according to the number of parameters p it possesses (Akaike, 1974). More precisely, a model that maximizes the value

$$AIC = 2\ell - 2p \tag{C.3}$$

is considered to best represent the statistical structure of the data. However, it was found that this powerful criterion is not directly applicable to the mixture model cluster analysis due to the structural degeneracy existing in the parameter space of the mixture distribution (Lindsay, 1995; Bozdogan & Sclove, 1984). It has been proposed that the AIC should be modified by multiplying the penalty by a factor of 3/2, and therefore considering the quantity

$$AIC' = 2\ell - 3p, \tag{C.4}$$

whose effectiveness has been tested for several examples (Bozdogan, 1992; Banfield & Raftery, 1993). This modified rule may provide an appropriate method of comparing mixture models with different numbers of components. In the one-dimensional multicomponent gaussian distributions, a distribution with m components would be considered superior to a distribution of $m - 1$ components only if its log likelihood is larger by at least $3 \times 3/2 = 4.5$, because adding one more component implies adding three parameters $\{w_k, \mu_k, \sigma_k^2\}$.

We fitted gaussian mixture distributions to the L_V distributions of the four areas. We found that the log likelihood of the two-component gaussian mixture distribution is greater than that obtained with the one-component gaussian distribution by 128.6, 63.2, 126.3, and 24.3, respectively, for the pre-SMA, SMA, CMAr, and PF. These differences are much greater than 4.5, and hence we conclude that in each case, the two-component distribution is superior.

In changing from two components to three components, the log-likelihood values increase by 19.7, 18.5, 25.5, and 0.2, respectively. According to our criterion, this implies that for the first three areas, the three-component distribution is superior. However, the data (approximately 1000 datum points in total) are not completely independent, because they are taken from a group of about 30 neurons, and for any given neuron, the spike sequences it generates all tend to have similar values of L_V. In such a situation, increasing the number of components may increase the sensitivity to the selection of the actual neurons studied. In accord with this observation, we found that the centers of the three components obtained for the fitted three-component gaussian distribution differ significantly among three areas. For this reason and because a single two-component distribution is able to fit the data for the pre-SMA, SMA, and CMAr simultaneously, we employed the two-component distribution.

Appendix D: Peri-Event Population Histograms

To study the possibility that neurons belonging to type A and type B (or type A′ and type B′) may exhibit different types of activity in response to external stimuli, we constructed peri-event population histograms separately for

these two groups of neurons in each area (see Figure 5). For each spike sequence obtained, if the number of spikes (in the waiting period) exceeds 100, we select the centrally located 100 consecutive ISIs to compute the value of L_V. If the mean value of L_V for all the sequences generated from a neuron is greater than $\theta = 0.59$ ($\theta' = 0.66$), this neuron (as are all the sequences generated from it) is classified as type A (A'), and otherwise as type B (B').

The bin size for the peristimulus histograms in Figure 5 was taken as 50 msec. The possible deviation from the temporal spike rate obtained for each bin of the population histograms is estimated as follows. The total number of spike sequences satisfying the above-mentioned conditions was about 1000 for each area, and the numbers of type A sequences and type B sequences selected accordingly were approximately the same: nearly equal to 500. Because the mean spike rate was about 30 spikes per sec, the number of spikes accumulated in each bin was about $30 \times 0.05 \times 500 = 750$. The two-sided possible deviation at a significance level of 0.05 is estimated as 1.96 times the standard deviation (which is $750^{1/2} \approx 27$ in the present case). The possible deviation at a significance level of 0.05 measured in units of the spike rate is therefore estimated as $30 \times 27/750 \times 1.96 \approx 2$ spikes per sec.

It is, of course, desirable to measure the evolution of individual neuronal activity to determine the response latency of each neuron. Because the typical number of spike sequences obtained from a single neuron is about 40 in the experiment, the statistical deviation estimated in the manner described above is about 8 spikes per sec, which is too large to allow for the detection of any systematic tendency. If we wish to decrease the statistical deviation of these data to the level of 2 spikes per sec, the bin size of the peri-event histogram should be enlarged to 0.6 sec, which is too coarse to determine the latency period. For these reasons, the histograms were constructed for spike sequences over ensembles of neurons.

Appendix E: Determination of Latencies

The spike rates of the two groups of neurons in the pre-SMA change in response to the stimulus LED. In order to determine the corresponding transition time, we fit the piecewise linear function,

$$f(t) = \begin{cases} c, & \text{for } t < a \\ c + b(t - a), & \text{for } t \geq a, \end{cases} \tag{E.1}$$

to the set of spiking data (or to peristimulus histograms with a small time bin). The least square fit of $f(t)$ to the data corresponds to the maximum likelihood estimate with the assumption of gaussian distribution around the fitting function. With this maximum likelihood method, we can estimate the most probable parameter values and the range of possible deviation with a given significance level.

We fitted $f(t)$ to type A data on the interval $-250 < t < 300$ msec and to type B data on the interval $-250 < t < 250$ msec for the pre-SMA (see Figure 6A), as these data do not exhibit saturation in these periods. With a least-square fit, the transition times were determined to be $a = 131$ msec and $a = 43$ msec, respectively, for type A and type B groups. From the log-likelihood values, the possible statistical deviations of these values of a are both estimated to be about ± 14 msec at a significance level of 0.05 and about ± 20 msec at a significance level of 0.01. Therefore, the presence of time difference between the two peristimulus responses is statistically significant.

We also fitted $f(t)$ to the type A and type B data, which are subclassified further according the waiting period 8 and 4 sec (see Figures 6B–6E). The transition times are estimated as 46 ± 15 msec for the type B sequences with the waiting period of 8 sec, 40 ± 27 msec for type B of 4 sec, 134 ± 22 msec for type A of 8 sec, and 120 ± 31 msec for type A of 4 sec. The statistical deviations, estimated at a significance level of 0.05, increased from those of the original data, as the data are reduced by the subdivision. In the task considered here, the latencies do not change according to the choice of the waiting period, while those of type A data and type B data are kept mutually distinguishable.

References

Akaike, H. (1974). A new look at the statistical model identification. *IEEE Trans. Autom. Contr. AC-19*, 716–723.

Bak, M.J., & Schmidt, E. M. (1977). An improved time-amplitude window discriminator. *IEEE Trans Biomed Eng., 24*, 486–489.

Banfield, J. D., & Raftery, A. (1993). Model-based gaussian and non-gaussian clustering. *Biometrics, 49*, 803–821.

Bozdogan, H. (1992). Choosing the number of component clusters in the mixture-model using a new informational complexity criterion of the inverse-Fisher matrix. In O. Opitz, B. Lausen, & R. Kler (Eds.), *Information and Classification, Proceedings of the 16th Annual Conference of the Gesellschaft Klassifikation e.V* (pp. 40–54). New York: Springer-Verlag.

Bozdogan, H., & Sclove, S. L. (1984). Multi-sample cluster analysis using Akaike's information criterion. *Annals of the Institute of the Statistical Mathematics, 36*, 163–180.

Buzsaki, G., Leung, L. S., & Vanderwolf, C. H. (1983). Cellular bases of hip-pocampal EEG in the behaving rat. *Brain Research Reviews, 6*, 139–171.

Constantinidis, C., Williams, G. V., & Goldman-Rakic, P. S. (2002). A role for inhibition in shaping the temporal flow of information in prefrontal cortex. *Nature Neuroscience, 5*, 175–180.

Csicsvari, J., Hirase, H., Czurko, A., & Buzsaki, G. (1998). Reliability and state dependence of pyramidal cell-interneuron synapses in the hippocampus: An ensemble approach in the behaving rat. *Neuron, 21*, 179–189.

Evarts, E. V. (1968). A technique for recording activity of subcortical neurons in moving animals. *Electroencephalogr. Clin. Neurophysiol., 24*, 83–86.

Fuster, J. M. (1997). *The prefrontal cortex: Anatomy, physiology, and neuropsychology of the frontal lobe.* New York: Lippincott-Raven.

Garey, L. (1999). *Broadmann's localisation in the cerebral cortex.* London: Imperial College Press.

Holt, G. R., Softky, W. R., Koch, C., & Douglas, R. J. (1996). Comparison of discharge variability in vitro and in vivo in cat visual cortex neurons. *J. Neurophysiology, 75*, 1806–1814.

Lindsay, B. G. (1995). *Mixture models: Theory, geometry and applications.* Hayward, CA: Institute of Mathematical Statistics.

Parent, A. (1996). *Carpenter's human neuroanatomy* (9th ed.). Baltimore, MD: Williams & Wilkins.

Ranck, J. B., Jr. (1973). Studies on single neurons in dorsal hippocampal forma-tion and septum in unrestrained rats. Part I. Behavioral correlates and firing repertoires. *Exp. Neurol., 41*, 461–531.

Sakai, Y., Funahashi, S., & Shinomoto, S. (1999). Temporally correlated inputs to leaky integrate-and-fire models can reproduce spiking statistics of cortical neurons. *Neural Networks, 12*, 1181–1190.

Shima, K., Sawamura, H., & Tanji, J. (2001). Neuronal activity in the supple-mentary and pre-supplementary motor areas in a multiple waiting-period task. In *Proc. 31st Annu. Soc. Neurosci* (p. 1932). San Deigo, CA: Society for Neuroscience.

Shima, K., & Tanji, J. (2000). Neuronal activity in the supplementary and presup-plementary motor areas for temporal organization of multiple movements. *J. Neurophysiol., 84*, 2148–2160.

Shinomoto, S., Sakai, Y., & Funahashi, S. (1999). The Ornstein-Uhlenbeck process does not reproduce spiking statistics of neurons in prefrontal cortex. *Neural Computation, 11*, 935–951.

Shinomoto, S., Shima, K., & Tanji, J. (2002). New classification scheme of cortical sites with the neuronal spiking characteristics. *Neural Networks, 15*, 1165–1169.

Shinomoto, S., & Tsubo, Y. (2001). Modeling spiking behavior of neurons with time-dependent Poisson processes. *Phys. Rev. E*, 041910 (1–13).

Tanji, J. (1996). New concepts of the supplementary motor area. *Curr. Opin. Neurobiol., 6*, 782–787.

Tiesinga, P .H. E., Fellous, J. M., & Sejnowski, T. J. (2002). Attractor reliability reveals deterministic structure in neuronal spike trains. *Neural Computation, 14*, 1629–1650.

This article has been cited by:

2. Hideaki Shimazaki, Shigeru Shinomoto. 2007. A Method for Selecting the Bin Size of a Time Histogram. *Neural Computation* **19**:6, 1503-1527. [Abstract] [PDF] [PDF Plus]

3. Keiji Miura, Masato Okada, Shun-ichi Amari. 2006. Estimating Spiking Irregularities Under Changing Environments. *Neural Computation* **18**:10, 2359-2386. [Abstract] [PDF] [PDF Plus]

4. Kazushi Ikeda . 2005. Information Geometry of Interspike Intervals in Spiking Neurons. *Neural Computation* **17**:12, 2719-2735. [Abstract] [PDF] [PDF Plus]